Sparse unmixing analysis for hyperspectral imagery of space objects

Zhenwei Shi[a], Xinya Zhai[a], Durengjan Borjigen[b], Zhiguo Jiang[a]
[a]Image Processing Center, School of Astronautics, Beihang University, Beijing 100191, China
[b]School of Mathematics and Systems Science, Beihang University, Beijing 100191, China

ABSTRACT

Spectral unmixing analysis for hyperspectral images aims at estimating the pure constituent materials (called endmembers) in each mixed pixel and their corresponding fractional abundances. In this article, we use a semi-supervised approach based on a large spectral database. It aims at finding the optimal subset of spectral signatures in a large spectral library that can best model each mixed pixel in the scene and computes the fractional abundance which every spectral signal corresponds to. We use $l_2 - l_1$ sparse regression technical which has the advantage of being convex. Then we adopt split Bregman iteration algorithm to solve the problem. It converges quickly and the value of regularization parameter could remain constant during iterations. Our experiments use simulated pure and mixed pixel hyperspectral images of Hubble Space Telescope. The endmembers selected in the solution are the real materials' spectrums in the simulated data and the approximations of their corresponding fractional abundances are close to the true situation. The results indicate the algorithm works well.

Key words: Sparse unmixing, space object, endmember, fractional abundance

1. INTRODUCTION

With more and more spacecrafts around the earth, it's necessary for many countries to monitor them. Space remote sensing imagery involves the acquisition of information from the spacecrafts' surface without physical contact with the area under study. Among the remote sensing modalities, hyperspectral imaging has recently emerged as a powerful technology. The imaging spectrometer simultaneously scans the same surface scenery at dozens even hundreds spectral bands [1]. Hyperspectral images contain rich spectral information to identify and recognize the materials. However, mixed pixels are widespread in hyperspectral images, due to insufficient spatial resolution and unavailability of completely pure spectral signatures in the scene. It becomes an obstacle to quantification analysis.

To deal with the mixture problem, linear spectral mixture analysis technique first identifies a collection of pure constituent spectra in the literature [2], and then expresses the measured spectrum of each mixed pixel as a linear combination of endmembers weighted by fractions or abundances that indicate the proportion of each endmember present in the pixel. Several hyperspectral unmixing methods have been proposed in recent years, which include N-FINDR[3], vertex component analysis[4], independent component analysis[5], the minimum volume enclosing simplex algorithm[6] and flexible similarity measures[7] and nonnegative matrix factorization (NMF)[8,9]. All the algorithms above can be separated into two categories: one is to select endmembers first and then solve the abundances; another is to solve both endmembers and abundances directly from the data. They face the same two problems: one is how many endmembers contained in the hyperspectral image, and the other is what kind of materials the endmembers are. It is difficult to confirm the number of endmembers from the data itself. For the second problem, we can solve it to some extent by measuring the similarity between endmembers and the spectrums of pure materials in spectral libraries. To avoid the problems and simplify the unmixing process, we assume there is a large enough spectral library which contains all the endmembers and other materials. In this paper, we adopt a semi-supervised approach using a spectral library to solve the abundances of all the material in spectral database and to select endmembers automatically. To prove our algorithm is efficient, we adopt simulated data whose endmembers and their fractional abundances we know in advance.

The structure of the paper is as follows: In Section 2 we establish the sparse unmixing model and then use split Bregman iteration algorithm [11] to solve the problem in Section 3. At last we evaluate our method by experiments on both pure and mixed pixel simulated hyperspectral images in Section 4 and close with conclusion in Section 5.

International Symposium on Photoelectronic Detection and Imaging 2011: Space Exploration Technologies and Applications, edited by John C. Zarnecki, Carl A. Nardell, Rong Shu, Jianfeng Yang, Yunhua Zhang, Proc. of SPIE Vol. 8196, 81960Y · © 2011 SPIE · CCC code: 0277-786X/11/$18 · doi: 10.1117/12.900271

2. SPARSE UNMIXING MODEL

Many algorithms use linear mixing model to solve unmixing problem. It corresponds to a reasonable balance between accuracy and model complexity. It assumes that a spectrum from a given pixel is a linear combination of the spectra of material present in the pixel. The coefficients are fractional abundances of corresponding spectrums. For each pixel, it can be expressed as follows:

$$v = \sum_{i=1}^{P} h_i w_i + n = Wh + n \quad (1)$$

Where v is a $L-by-1$ column vector (the measured spectrum of a pixel), L is the number of spectra bands, P is the number of endmembers, h_i is the fractional abundance of the i^{th} endmember, w_i is the spectrum of i^{th} endmember, n is a $L-by-1$ vector collecting the errors affecting the measurements at each spectral band. W is a $L-by-P$ endmember matrix, and h is a $P-by-1$ vector of abundance.

The fractional abundances of the endmembers sum to one and can not be negative. These constrains are known as the sum-to-one and the non-negativity constraints:

$$\sum_{i=1}^{P} h_i = 1 \text{ (sum-to-one)} \quad (2)$$

$$h_i \geq 0, \forall i \text{ (non-negativity)} \quad (3)$$

We put pixels of all columns in a line. Then the hyperspectral data cube changes into 2-D matrix in which the column represents spectra dimension and the row represents space dimension. The linear mixing model in the form of matrix is:

$$V = WH \quad (4)$$

Where V is a $L-by-K$ matrix, and H is a $P-by-K$ matrix. K is the number of pixels of hyperspectral image. According to every row vector in H, we can get the distribution of each endmember in hyperspectral images.

Here, we use linear mixing model in a semi-supervised approach, where a matrix S containing many spectrums from spectral library takes place of W. It can be written as:

$$V = SH \quad (5)$$

Where S is a $L-by-Q$ spectra matrix, and H is a $Q-by-K$ abundance matrix. Here, $Q > P$ and $Q >> L$. Thus, it has many solutions of H as it is an underdetermined system. As the number of pure materials containing in each pixel is much less than in the spectral library, H is sparse. We can obtain a sparse unique solution using an efficient sparse regression technique. A very simply and intuitive measure of sparsity of H is the l_0 norm $\|H\|_0$ which denotes the number of nonzero components of the matrix .The sparse unmixing problem is:

$$\min_H \|H\|_0 \qquad s.t.\ \ SH = V \quad (6)$$

The unconstrained minimization problem is:

$$\min_H \left\{ \frac{1}{2} \|V - SH\|_2^2 + \lambda \|H\|_0 \right\} \quad (7)$$

This is a classical problem of combination search which sweeps exhaustively through all possible sparse subsets. The complexity of exhaustive search is exponential in Q and it is NP-hard. The objective function is a non-convex, difficult to solve. However, for the matrix S with certain properties of incoherence, the l_0 norm of sparse matrix H can be replaced by the l_1 norm $\|H\|_1$:

$$\min_H \left\{ \frac{1}{2}\|V - SH\|_2^2 + \lambda \|H\|_1 \right\} \tag{8}$$

Here, $\|H\|_1 = \sum_{i=1}^{q} \sum_{j=1}^{K} |H_{i,j}|$.

It is a l_1 minimization problem and can be solved by some standard convex optimal algorithms. Here we use split Bregman iteration.

3. SPLIT BREGMAN ITERATION ALGORITHM

Split Bregman iteration algorithm was first introduced by Goldstein and Osher for solving total variation (TV), compress sensing and other regularized problems [11]. To solve the unconstrained sparse reconstruction problem, the iteration is generated by using an auxiliary variable D and given by

$$\min_{H,d} \frac{1}{2}\|V - SH\|_2^2 + \lambda \|D\|_1 \quad s.t. \; D = H \tag{9}$$

Convert it into an unconstrained problem:

$$\min_{H,d} \lambda \|D\|_1 + \frac{\mu}{2}\|V - SH\|_2^2 + \frac{1}{2}\|D - H\|_2^2 \tag{10}$$

The regularized parameters λ, μ work as penalties balancing the energy functions. Optimization problem (10) is performed in an alternating fashion:

$$\begin{cases} H^{k+1} = \arg\min \left\{ \frac{\mu}{2}\|V - SH\|_2^2 + \frac{1}{2}\left\|D^k - H - B^{k+1}\right\|_2^2 \right\} \\ D^{k+1} = \arg\min \left\{ \lambda \|D\|_1 + \frac{1}{2}\left\|D - H^{k+1} - B^{k+1}\right\|_2^2 \right\} \end{cases} \tag{11}$$

Where k denotes the iteration step.

In this fashion, we "split" the l_1 and l_2 components of minimization function. B^k comes from adding back the error.

Then we can perform this minimization scheme as follows: initially set $H^0 = B^0 = D^0 = 0; V^0 = V$, and then update the variables by iterations. The iteration is given as:

$$\begin{cases} H^{k+1} = (\mu S^T S + I)^{-1}(\mu S^T V^k - B^k + D^k) \\ D^{k+1} = \max(H^{k+1} + B^k - \lambda, 0) \\ B^{k+1} = B^k + H^{k+1} - D^{k+1} \\ V^{k+1} = V^k + V - SH^{k+1} \end{cases} \tag{12}$$

As $\left\|H^{k+1} - H^{k}\right\|_2 < tol$, where tol is the tolerance limit, the iteration stops. If the iteration stops with only few steps, we use a fixed number of iterations. λ and μ are determined by the actual data. The experiments following show it is a very efficient method for l_1 minimization.

4. EXPERIMENTS ON SIMULATED HYPERSPECTRAL IMAGES OF SPACE OBJECTS

For our numerical tests, we use the data developed by Zhang et al. [12], where the authors constructed a dataset of simulated data using a 3-D model of Hubble Space Telescope and a NASA library of material spectral signatures. The simulated hyperspectral image consists of 8 materials which were assigned based on orientation of the Hubble telescope. Their spectrums cover a band of spectrum from $0.4\mu m$ to $2.5\mu m$ for 100 evenly distributed sampling points, leading to a hyperspectral data of size 193*177*100.

Figure 1 shows the first band hyperspectral image of Hubble Satellite Telescope. Figure 2 and Figure 3 show the spectral signatures of 8 endmembers and their distributions in the image, respectively.

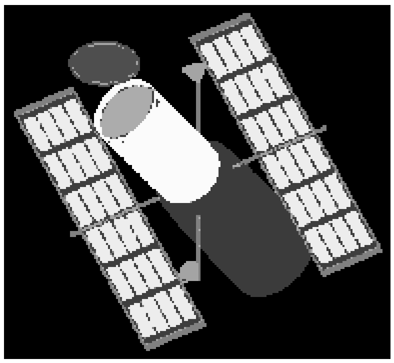

Figure 1. Simulated Hubble Satellite Telescope hyperspectral image of band 1

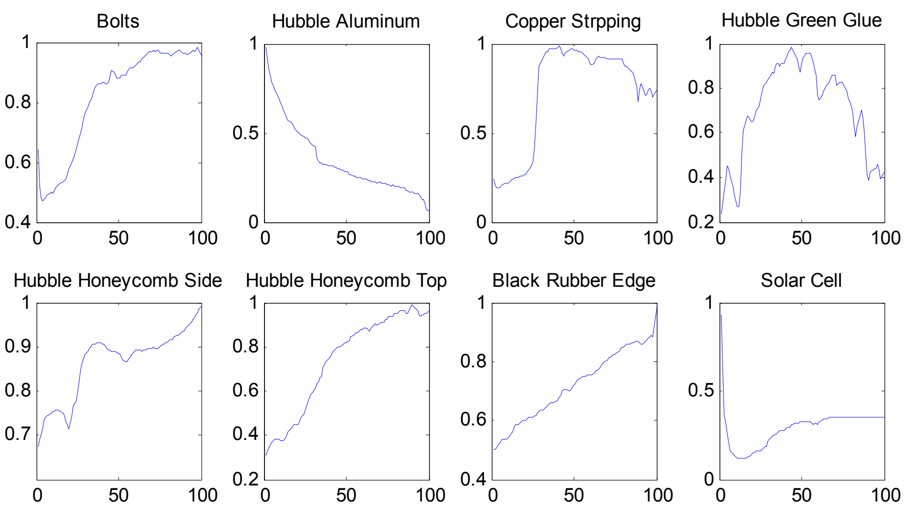

Figure 2. Spectral signatures of 8 pure materials designed in simulated data

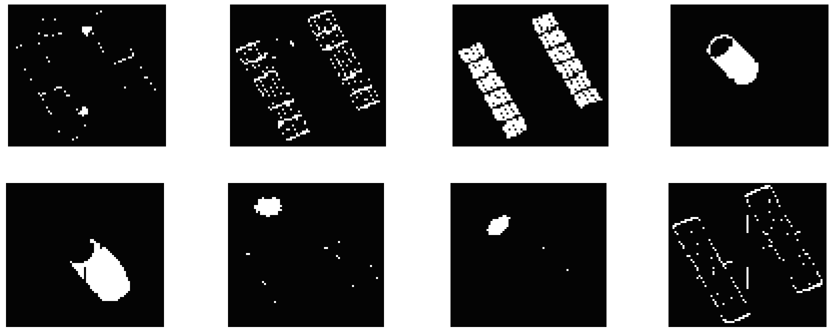

Figure 3. Space distribution of 8 endmembers in simulated data

We designed the fractional abundances of 8 materials in every pixel, pure or mixed. By using the formula (5), the simulated data is obtained.

The spectral library matrix S used in experiments was generated from USGS digital spectral library. We select 599 spectrums with 224 spectral bands distributed uniformly in the interval $0.4-2.5\mu m$. Here we resample the spectra and decrease spectral bands checking with spectrums of 8 component materials. Then spectral matrix S is $100-by-599$ size. Here we set $\mu=\frac{100}{\left\|S^T S\right\|_2}$, and $\lambda=0.05$. We test our algorithm with pure and mixed pixel simulated data.

4.1 Pure pixel hyperspectral images

In the pure simulated data, every pixel contains only one material at most, and the fractional abundances of all the pixels are 0 or 1. The RMSE (root mean square error) of the solution is 7.9×10^{-4} with 500 step iterations.

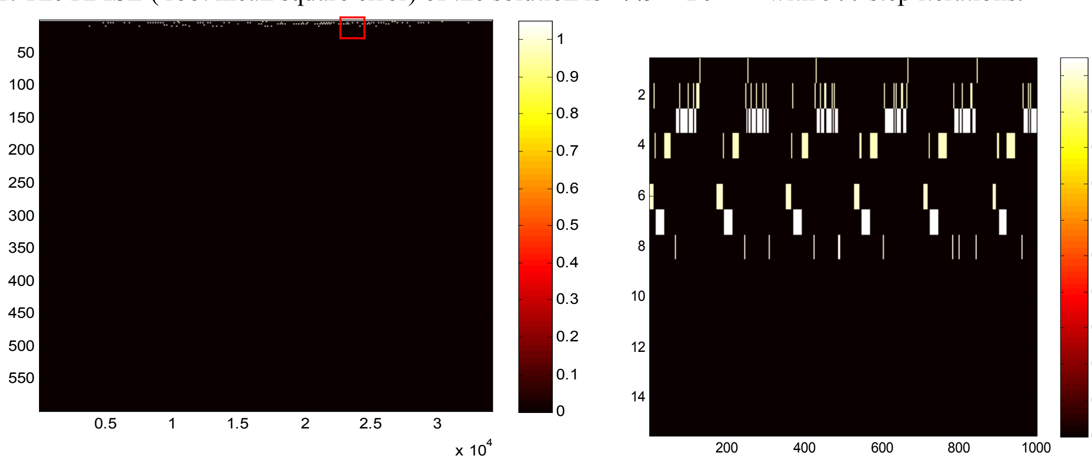

(a) (b)

Figure 4. The sparse unmixing result of pure data (a) The solved fractional abundance matrix of the result valued by colors (b) Details of the labeled region in (a).

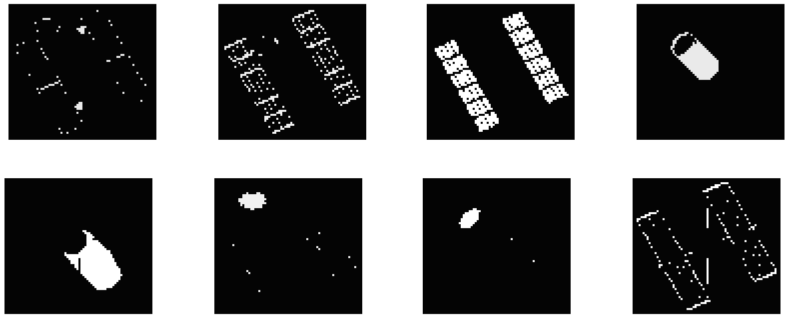

Figure 5. Fractional abundances solved of 8 endmembers in pure data

Figure 4 illustrates the solution of our algorithm is sparse. In figure 5, we map the rows in abundance matrix whose values are non-zero. It's clear that the solution is close to the true condition by comparing figure 3 and figure 5.

4.2 Mixed pixel hyperspectral images

We reduce the space resolution of the simulated hyperspectral image to a quarter of origin to create the mixed simulated data. Each pixel consists of several materials whose fractional abundances sum to one. It's more complicated than pure pixel condition and needs more iteration steps to converge. The result is that RMSE is 0.0013 with 500 iteration steps and 6.15×10^{-4} with 1000 iteration steps. The same as figure 4, figure 6 shows fractional abundance matrix is sparse. Figure 7 and figure 8 illustrate the solution closes to the fractional abundance designed.

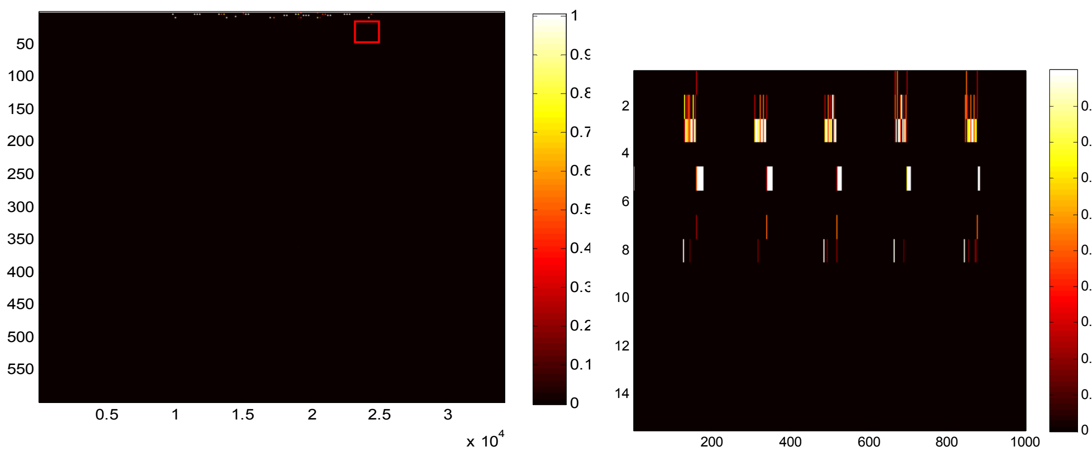

(a) b)

Figure 6. The sparse unmixing result of mixed data (a) The fractional abundance matrix of the result valued by colors (b) Details of the labeled region in (a)

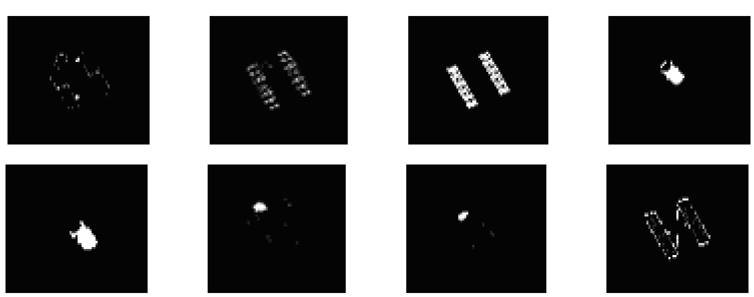

Figure 7. Fractional abundances designed of 8 endmembers in mixed data

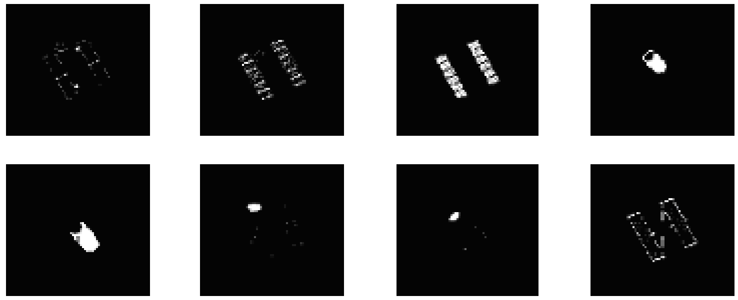

Figure 8. Fractional abundances solved of 8 endmembers in mixed data

5. CONCLUSIONS

The paper introduces $l_2 - l_1$ sparse regression technical to unmix hyperspectral images of space objects and applying split Bregman method to solve the minimization problem. The experimented results show our algorithm succeeds in solving fractional abundances in both pure and mixed simulated hyperspectral images and also it selects the true endmembers from a large spectral library. The unmixing process is the procedure to identify the components of the surface of space objects. We will have a further study on robust unmixing methods in the field of identification of space objects.

ACKNOWLEDGMENTS

The work was supported by the National Natural Science Foundation of China under the Grants 60975003, the 973 Program under the Grant 2010CB327904, the Fundamental Research Funds for the Central Universities under the Grant YWF-10-01-A10, and the Beijing Municipal Natural Science Foundation under the Grant 4112036.

REFERENCES

[1] Green R. O., Eastwood M. L., Sarture C. M., Chrien T. G., Aronsson M., Chippendale B. J., Faust J. A., Pavri B. E., Chovit C. J., and Solis M., "Imaging spectroscopy and the airborne visible/infrared imaging spectrometer(AVIRIS)", Remote Sensing of Environment, 65(3),227–248(1998).

[2] Plaza A., Martinez P., Perez R., and Plaza J., "A quantitative and comparative analysis of endmember extraction algorithms from hyperspectral data", IEEE Transactions on Geoscience and Remote Sensing, 42(3), 650–663(2004).

[3] Winter M. E., "N-FINDR: An algorithm for fast autonomous spectral end-member determination in hyperspectral data", In Proc. SPIE Conf. Imaging Spectrometry V, 266–275(1999).

[4] Nascimento J. M. P. and Dias J. M. B., "Vertex component analysis: A fast algorithm to unmix hyperspectral data", IEEE Transactions on Geoscience and Remote Sensing, 43(4): 898–910(2005).

[5] Wang J. and Chang C. I., "Applications of independent component analysis in endmember extraction and abundance quantification for hyperspectral imagery", IEEE Transactions on Geoscience and Remote Sensing, 44(9): 2601–2616, (2006).

[6] Chan T. H., Chi C. Y., Huang Y. M., and Ma W. K., "A convex analysis-based minimum-volume enclosing simplex algorithm for hyperspectral unmixing", IEEE Transactions on Geoscience and Remote Sensing, 47 (11): 4418–4432(2009).

[7] Chen J., Jia X., Yang W., and Matsushita B., "Generalization of subpixel analysis for hyperspectral data with flexibility in spectral similarity measures", IEEE Transactions on Geoscience and Remote Sensing, 47(7): 2165–2171(2009).

[8] Paatero P. and Tapper U., "Positive matrix factorization: an on-negative factor model with optimal utilization of error estimates of data values", Environmetrics, 5:111–126(1994).

[9] Lee D. D. and Seung H. S., "Learning the parts of objects by non-negative matrix factorization", Nature, 401:788–791(1999).

[10] Bruckstein A. M., Donoho D. L., and Elad M., "From sparse solutions of systems of equations to sparse modeling of signals and images", SIAM Review, 51:34–81(2009).

[11] Goldstein T., and Osher S., "The split Bregman method for l1 regularized problems", SIAM Journal on Imaging Sciences, 2(2), 323-343(2009).

[12] Zhang Q., Wang H., Plemmons R., and Pauca P., "Tensor Methods for Hyperspectral Data Analysis: A Space Object Material Identification Study", Journal of the Optical Society of America, A., 25(12), 3001-3012(2008).